Peer-Reviewed Technical Communication

Direct Measurements of Sediment Sound Speed and Attenuation in the Frequency Band of 2–8 kHz at the Target and Reverberation Experiment Site

Jie Yang and Dajun Tang

***Abstract*—The sediment acoustic-speed measurement system is designed to measure *in situ* sediment sound speed and attenuation within the surficial 3 m of sediments in the frequency band of 2–8 kHz. Measurements were carried out during the Target and Reverberation EXperiment 2013 (TREX13) off Panama City, FL, USA. During TREX13, nine deployments at five selected sites were made along the 20-m isobath, termed the main reverberation track. The sediment types at the five selected sites ranged from coarse sand to a mixture of soft mud over sand, and the measured results show a spread of 80 m/s in sediment sound speed among the different types of sediments for all frequencies. Between 2–8 kHz, about 3% dispersion was observed at the sandy sites, whereas little dispersion was observed at the sites with mud. Preliminary attenuation results show 0.5–3.3 dB/m at the sandy sites, and 0.5–1.0 dB/m at the sites with mud in the same frequency band.**

***Index Terms*—Dispersion, *in situ*, midfrequency, sediment sound speed and attenuation.**

I. Introduction

SEDIMENT sound speed and attenuation are important parameters for modeling sound propagation and reverberation in shallow water. These parameters can be measured with relative ease at high frequencies (>20 kHz). Those results, however, may not be directly used for midfrequency (1–10 kHz) applications because of their frequency dependency, which is most pronounced in the frequency band between several 100 Hz and a few kilohertz for sand [1], [2]. On the other hand, making *in situ* measurements in the field at midfrequencies is a challenging problem. Direct measurement of sediment geoacoustic properties by inserting sensors into sediments started in the 1950's [3]. There are generally three methods to deploy sensors into sediments: manual, gravitational, and controlled drill by a motor. Currently, most are limited to surficial measurements (<5 m). The manually buried acoustic systems are limited to water depths where diver support is available [4]–[6], and the burial depth is generally limited to less than 0.5 m. The other two types of systems can function in the general littoral oceans [7]–[12]. Among them, most systems [7]–[11] penetrate through gravitational force while Sediment Acoustic-speed Measurement System (SAMS) [12] uses a controlled drill, which can target penetration depth to centimeter resolution.

SAMS [12] is designed to measure sediment sound speed and attenuation simultaneously over the surficial 3 m of sediments. Fig. 1 shows a schematic of SAMS. The system is about 4.8 m tall and 5 m wide between the end points of the triangular base and the extension arm. It includes ten sources and among them nine are ITC1032 and one is ITC1007. These sources are placed on the triangular frame and the extension arm to provide different ray-paths to improve estimates of sediment parameters. Specifically, the ITC1007 is placed at the far end of the extension arm, which is about 3 m away from the center probe. There are six ITC1032 sources on the extension arm and three on the triangular frame. The lowest frequency signal that the ITC1007 and ITC1032 can reliably transmit is 2 kHz.

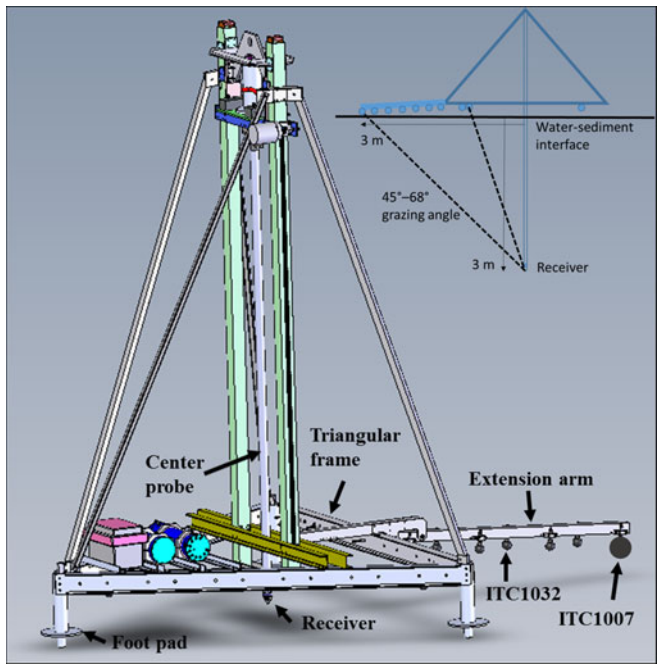

Fig. 1. SAMS: There are six ITC1032 and one ITC1007 sources on the extension arm and three ITC1032 on the triangular frame. A ring transducer (receiver) is at the tip of the center probe that is drilled into the sediment under motor control. The maximum penetration depth for the receiver is 3 m. Upper right corner: deployment geometry in TREX13 with receiver at a penetration depth of 3 m and sources extending 1–3 m horizontally from the center probe.

A single-ring transducer (receiver) is placed at the tip of the center probe that is driven into the seabed. SAMS has two independent and interchangeable drill systems: One employs a suction mechanism and the other a water jet. The suction system gives minimal disturbance to the medium around the penetrating probe while the water jet system can help penetrate consolidated shell/sand layers. A typical deployment lasts 15–30 min, as SAMS is lowered to the seafloor from a research vessel with dynamic positioning capability. Probe penetration and data acquisition are controlled on board the vessel.

Manuscript received December 22, 2016; revised April 20, 2017; accepted June 6, 2017. Date of publication July 11, 2017; date of current version October 11, 2017. This work was supported by the Office of Naval Research, Ocean Acoustics. *(Corresponding author: Jie Yang.)*

Associate Editor: N. Chotiros.

The authors are with the Applied Physics Laboratory, University of Washington, Seattle, WA 98105 USA (e-mail: djtang@apl.washington.edu).

Digital Object Identifier 10.1109/JOE.2017.2714722

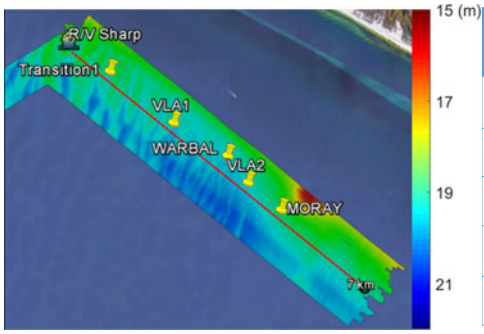

Location name	Latitude	Longitude
Transition1	30° 3.307'N	85° 40.412'W
VLA1	30° 2.785'N	85° 39.664'W
WARBAL	30° 2.451'N	85° 39.030'W
VLA2	30° 2.179'N	85° 38.789'W
MORAY	30° 1.902'N	85° 38.400'W

Fig. 2. SAMS deployment sites along the main reverberation track with their corresponding GPS locations.

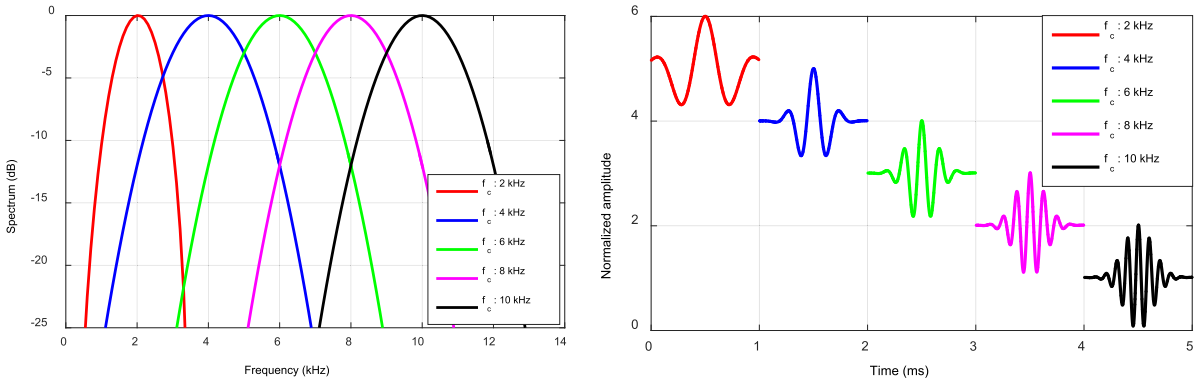

Fig. 3. Transmit signals: (a) spectra of five selected waveforms with center frequencies of 2, 4, 6, 8, and 10 kHz; and (b) their corresponding time domain waveforms shifted by 1 ms along the *x*-axis and unity along the *y*-axis between waveforms.

The Target and Reverberation EXperiment 2013 (TREX13) was carried out off the coast of Panama City, FL, USA. As part of the environmental characterization effort for TREX13, SAMS measurements were carried out from May 22–25 along the main reverberation track. The track is along the 20-m isobath at a 129° heading, about 2 km off shore. Measurements were taken at five representative sites, where sediment types range from coarse sand to mud over sand.

The water jet method was needed at the TREX13 site to penetrate to 3 m depth. Acoustic transmission covers the frequency band of 1–10 kHz with quality results in the band of 2–8 kHz. All data shown here were taken with the receiver at the maximum penetration depth of 3 m.

This paper is organized as follows. An overview of SAMS operation during TREX13 is given in Section II. The sediment sound speed and attenuation results are presented in Section III, followed by a summary in Section IV.

II. SAMS Operation During TREX13

A. TREX13 Experiment Description

Five representative sites were selected along the main reverberation track for direct measurements of sediment sound speed and attenuation. The five sites are named Transition1, VLA1, WARBAL, VLA2, and MORAY, which have varying sediment types from coarse sand, to fine sand, to soft mud over sand. A total of nine deployments were made, with two deployments per site except for Transition1, where there was only one. Fig. 2 shows the experimental area with the color panel representing the fine-scale bottom bathymetry from a multibeam survey [13], covering an area of 7 km × 1.2 km. The red line represents the center of the 7-km main reverberation track, starting about 500 m northwest of Transition1. Extensive acoustic and environmental measurements were taken along this track to support model/data comparisons for reverberation. The five SAMS deployment sites are labeled along the track in Fig. 2 with their corresponding GPS locations. The water depths of all deployments are 19–20 m.

The bathymetric data [13] show corrugations within the first 3 km of the track, from Transition1 to the WARBAL site. The peak-to-trough bathymetric variation of the corrugations is about 1 m. Along a corrugation, sediment composition changes from coarse sand on the ridge to mud over sand in the swale. Starting from the WARBAL site (3.6 km from the *R/V Sharp*), sediment starts transitioning into a relatively homogeneous fine sand.

Narrowband signals were transmitted at center frequencies of 1–10 kHz. Specifically, pulses with Gaussian envelopes were transmitted. Bandwidths of the pulses are 1 kHz for center frequencies lower than 3 kHz, and 2 kHz for center frequencies above 3 kHz. Five selected signals are shown in Fig. 3 with (a) showing their spectra and (b) their corresponding time domain waveforms with center frequencies of 2, 4, 6, 8, and 10 kHz. The transmitted signals are 1-ms-long pulses, with the peaks of their envelopes centering at the middle of the pulse.

B. Supporting Information for Sediment Composition and Potential Layering Structure

Multiple Go-pro cameras and a real-time camera feed were used during SAMS deployments, which provided seafloor images and helped identify materials that were flushed to the seafloor surface after jetting. In addition, as the SAMS receiver penetrated into the bottom, the penetration depth as a function of time was recorded. Since all deployments during TREX13 were carried out in the same way, i.e., the system was

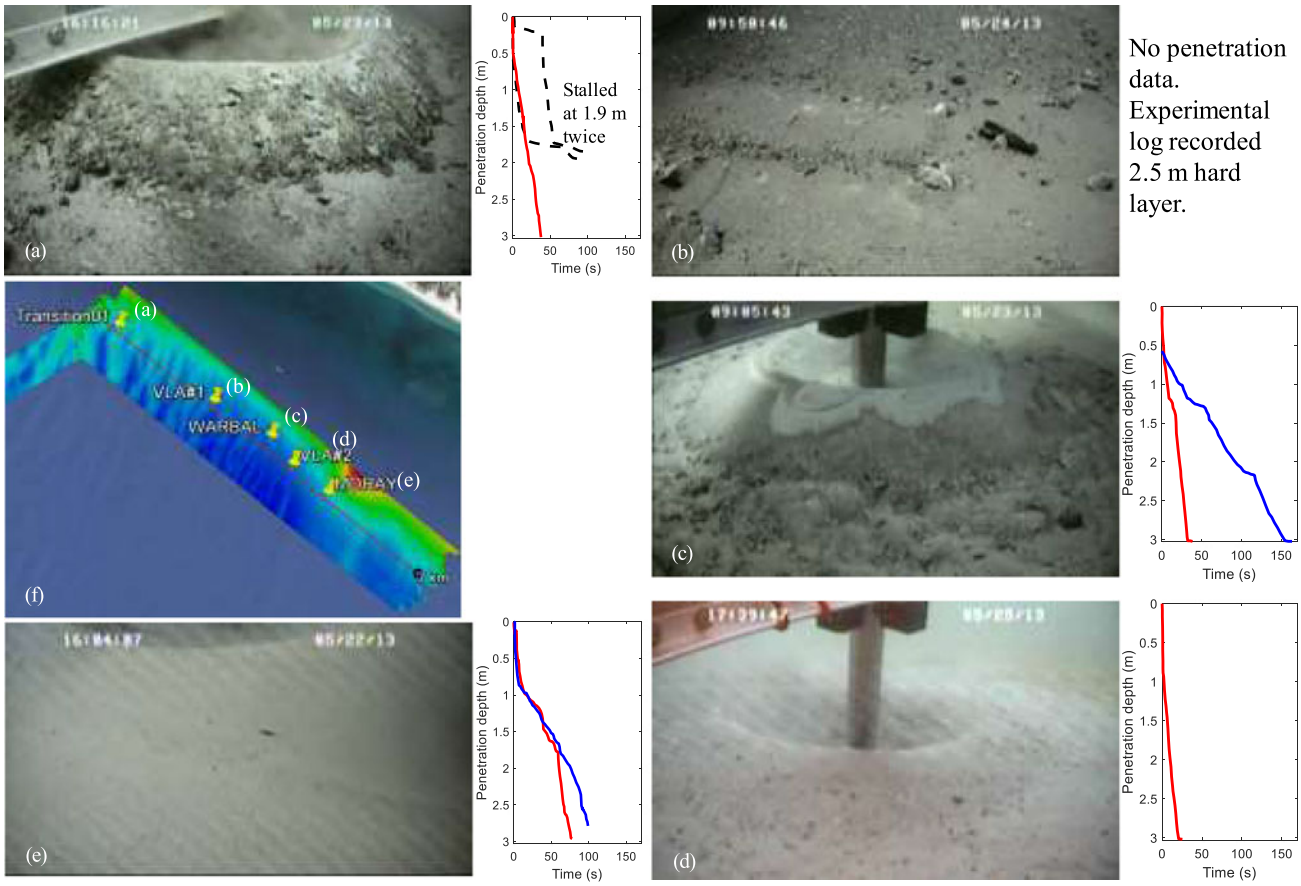

Fig. 4. (a)–(e) clockwise, underwater camera images after drilling down to 3 m with corresponding penetration depth data for the five selected sites; and (f) experiment location map. Different curves in the penetration depth data correspond to multiple deployments at the site. Solid lines: successful penetrations to 3 m. Dashed lines: unsuccessful penetrations.

left continuously drilling with constant water pressure of 20 lb/in^2, the decent rate and its variation indicate the level of difficulty in penetration and therefore, are indicators of sediment property change or layering structure.

Underwater camera images along with penetration rate data from each of the five sites are presented in Fig. 4. Clockwise, Fig. 4(a)–(e) corresponds to Transition1 down the main reverberation track to MORAY. Each panel has two parts, an image of surficial sediment taken after jetting and the penetration depth as a function of time. Fig. 4(f) is the site location map.

The underwater camera images are used to assess qualitatively the surficial sediment types for the five sites. The penetration depth data are discussed in terms of sediment property change and layering structure within the surficial 3 m. Finally, two deployments at VLA1 site are discussed, with one deployment sinking 30 cm into the surficial mud layer and the second made 20 m west of the first.

Observations from the images of the first two sites [Fig. 4(a) and (b)] show coarse sand and many shell fragments and small pebbles. The image at site WARBAL [Fig. 4(c)] clearly shows two different types of materials, one type much finer than the other. Surficial sediment at sites in Fig. 4(d) and (e), VLA2 and MORAY, where there is no apparent bathymetric corrugation [see Fig. 4(f)], shows homogeneous fine sand.

Penetration rate data show a possible hard layer at Transition1 and VLA1. At Transition1, two unsuccessful deployments [dashed lines in Fig. 4(a)], where the penetration process stalled at about 1.9 m, preceded the third successful deployment down to 3 m. Distance between

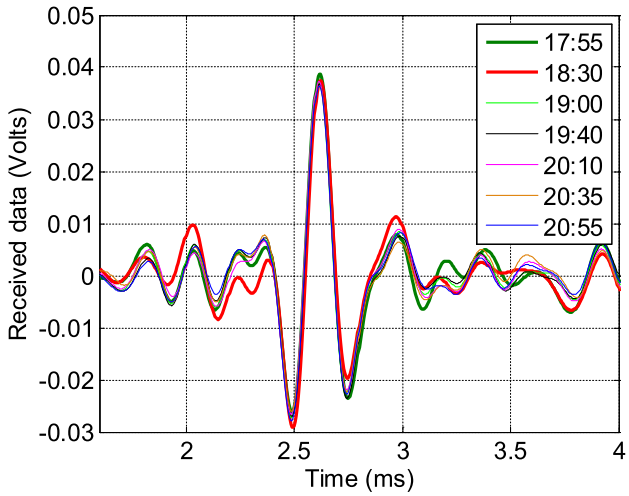

Fig. 5. Continuous recording of acoustic data over 3 h to observe signal stabilization using a 2-4 kHz Gaussian pulse. Legend shows local time at which data were taken. The first data set was taken at 17:55.

deployments is of O(10 m). One nearby vibracore, taken about 900 m to the NW of Transition1 near the *R/V Sharp* location, is available for comparison [14]. The vibracore penetrated the sediment to about 3 m and the split core shows a dense shell layer at 1.1–1.6 m depth, which may be the cause of a sub-bottom layering identified through

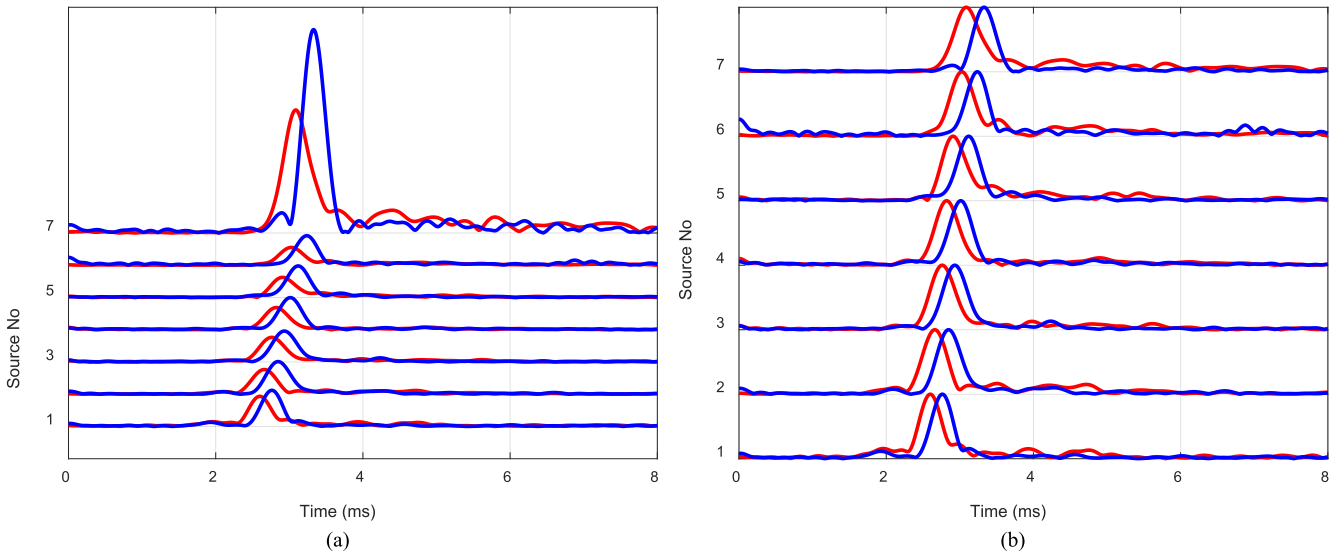

Fig. 6. Comparison of signal envelopes between in-water (blue) and in-sediment data (red) using a 1-ms, 2–4-kHz Gaussian pulse transmitted by the seven sources on the extension arm. (a) Both in-water and in-sediment data are normalized to the envelope peak of in-water data transmitted from source 1; and (b) data are uniformly normalized to envelope peaks of 1. Sources 1–6: ITC1032; source 7: ITC1007. Receiver at 3-m depth. *Y*-axis: source number. Source #1 is closest to the center probe, while #7 the furthest. #7, the ITC1007, has higher source level than those from the ITC1032 sources.

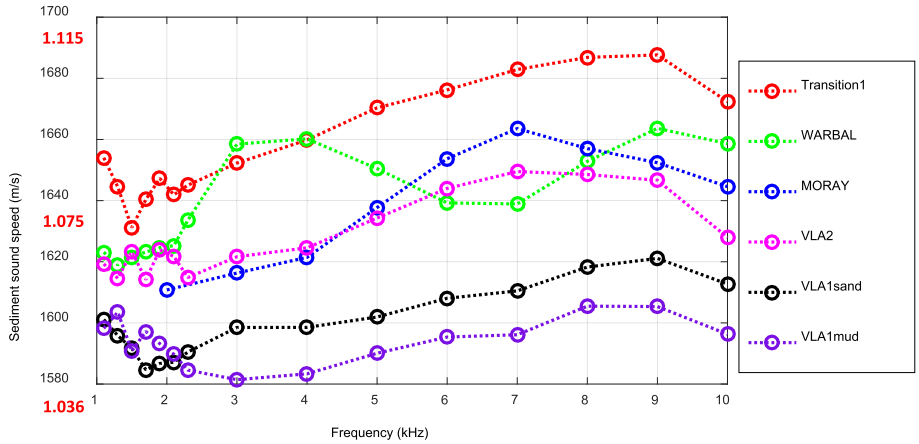

Fig. 7. Sediment sound speed results in the frequency band of 1–10 kHz at the five sites. Red numbers on the *y*-axis are sound speed ratios.

chirp profiling. This sub-bottom layer has a varying thickness of 1–3 m below the water–sediment interface and extends from the NW to the first 2–3 km of the main reverberation track [14]. This is consistent with the two unsuccessful penetrations to 1.9 m at Transition1 site.

For the VLA1 site, the probe also encountered penetration difficulty around 2.5 m but broke through after stalling for O(10 s). This is consistent with findings from a chirp sonar survey of a layer from Transition1 to VLA1 at about 2-m depth [14]. The two deployments at the WARBAL site show variable bottom properties, as one took 30 s and the other 150 s to penetrate. The significant difference in penetration time indicates changing sediment properties, although the two deployments were only O(10 m) apart. The image shown in Fig. 4(c) corresponds to the latter case where penetration took 150 s. Two types of sediment materials are clearly observable, indicating bottom layering structure. Although similar in surficial sediment types for VLA2 and MORAY, the penetration rate data at the MORAY site show a softer surficial layer of about 1 m, then a more consolidated sediment than at VLA2.

The two deployments at VLA1 reveal sediment property and structure changes. In the first deployment, SAMS sank about 30 cm into

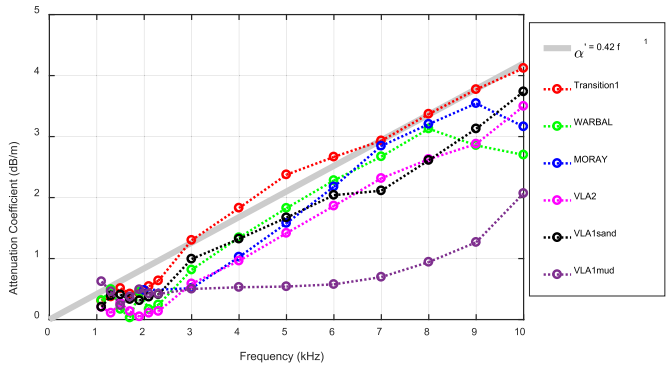

Fig. 8. Sediment attenuation coefficient in the frequency band of 1–10 kHz at the five sites. Reference line in gray: $\alpha' = 0.42 * f^1$, with α' the attenuation coefficient in decibel per meter [see (1)] and f the frequency in kilohertz.

the soft sediments and all sources were buried in mud. Small amounts of mud remained on the foot pads of the tower after retrieval. The

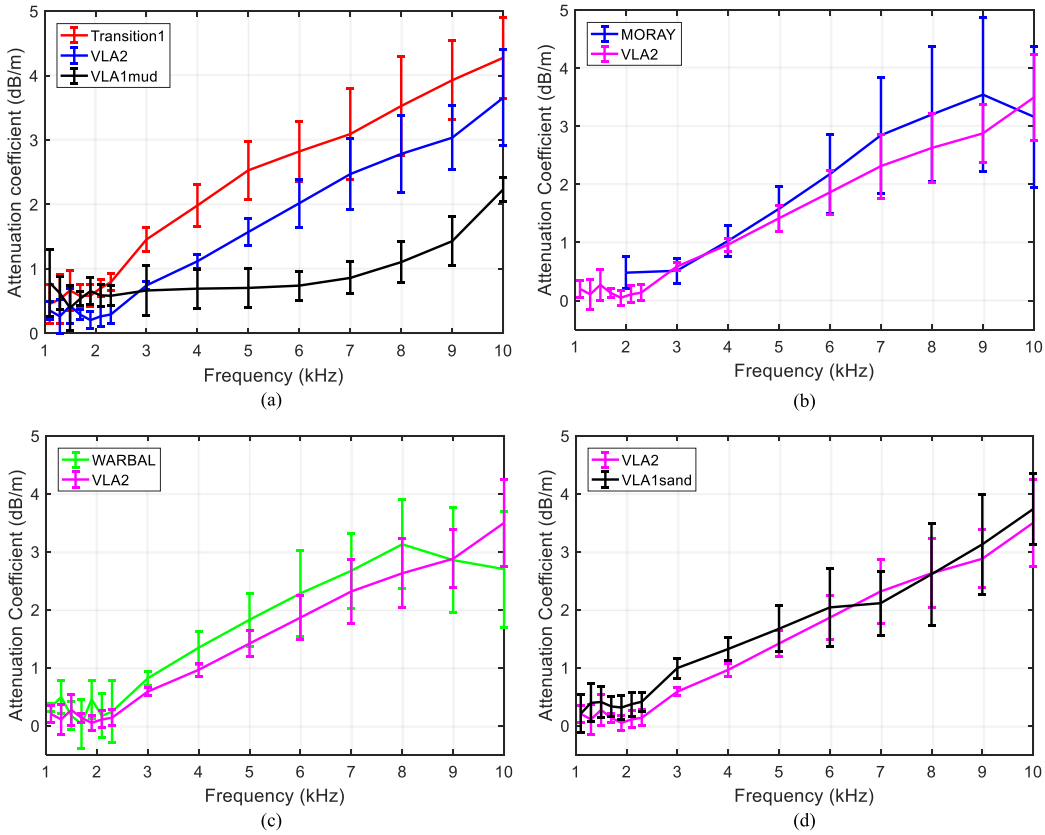

Fig. 9. Cross comparisons of sediment attenuation coefficient among the five sites: (a) Transition1, VLA2, and VLA1mud; (b) MORAY and VLA2; (c) WARBAL and VLA2; and (d) VLA2 and VLA1sand.

mud sample was congealable, e.g., it would retain its shape, however deformed, and had a consistency of wet cement to the touch. The second deployment was carried out 20 m to the west of the first deployment, where sediment was consolidated enough to support SAMS. The multibeam survey [13] shows that the spatial coverage of the exposed surficial mud is about 10–20 m, which was confirmed by divers. The difference in the two SAMS deployments at VLA1 is consistent with the multibeam and diver observations.

In summary, the five sites represent coarse sand (Transition1), fine sand (VLA2 and MORAY), sand with more complex bottom structure (WARBAL), and mud over sand (VLA1). Sediment sound speed and attenuation results (Section III) confirm the variation of sediment properties observed.

C. Assessing Sediment Disturbance

Because a water jet was used, effects of sediment disturbance by the jetting process were investigated. SAMS's center tube is about 3" in diameter. As shown in underwater camera pictures (see Fig. 4), the seafloor forms a small crater at the water–sediment interface caused by the waterjet, and it is less than 1 ft in diameter for all deployments.

To examine how long it would take for the disturbance to stabilize, acoustic data were continuously recorded for a few hours after penetration at Transition1. Acoustic data taken over 3 h are shown in Fig. 5. It takes about 1 h for the acoustic signal to stabilize. Interestingly, the main peak arrival is always stable, even immediately after a deployment. It is the smaller peaks that need more than one hour to stabilize. We assume that one hour after each deployment the disturbance caused by the water jet is restored to the prejetting condition. A minimum 1-h waiting time was used before taking acoustic measurements for all deployments in TREX13.

III. Sediment Sound Speed and Attenuation at the TREX13 Site

Acoustic signals from the five sites, covering the frequency band of 1–10 kHz, are used to determine sediment sound speed and attenuation. Sediment sound speed is obtained through a time-of-flight technique. To obtain sediment attenuation, a separate calibration data set, called in-water data, was acquired when the entire SAMS system was deployed in the water column with the same configuration as the deployments in sediments. By comparing the arrival amplitudes of in-water and in-sediment data and assuming the attenuation coefficient in water is negligible, a sediment attenuation coefficient is estimated. Results of TREX13 are also compared with those from the Sediment Acoustic Experiments 1999 and 2004 [1], [2].

A. Sediment Sound Speed Results

A comparison of signal envelopes of in-water and in-sediment data transmitted from the seven sources on the extension arm are shown in Fig. 6, with source 7 being the ITC1007 and the rest ITC1032 sources. The filtered in-water and in-sediment data are shown in blue and red, respectively, and both are taken under the same transmission/receiving configuration. The waveform is a Gaussian pulse in the band of 2–4 kHz. Fig. 6(a) and (b) shows the same data with different normalization schemes. In Fig. 6(a), all in-water and in-sediment signals were normalized by one number, which is the value at the peak of the envelope using the in-water signal transmitted from source 1.

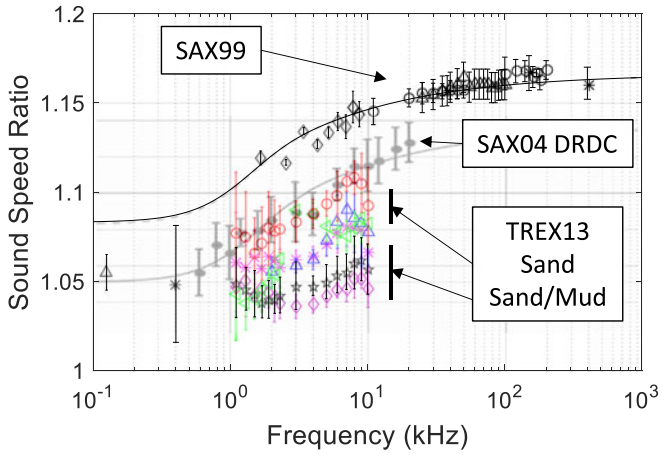

Fig. 10. Comparison of sediment sound speed ratio among TREX13 (colored), SAX99 (black), and SAX04 DRDC (gray). The TREX13 results are the mean sound speed results shown in Fig. 7 with uncertainty bounds. Top curve represents coarse sand to fine sand for the middle three curves; and the bottom two are sand/mud mixture.

This normalization preserves the relative amplitudes among all signals. In Fig. 6(b), data were uniformly normalized to envelope peak of one and this normalization helps display the trailing signal after the direct arrival. Signal arrival time is defined as the time difference between the envelope peaks of the received and transmitted signals. Peaks of the in-sediment data, as anticipated, arrive earlier and have lower amplitudes than those of the in-water data.

With known geometry of all sources and receiver relative to the water–sediment interface, the total propagation distances and the partial distances where sound travels in the sediment were calculated. In-water sound speed of 1528 m/s, measured by conductivity-temperature-depth profile (CTD), was used to calculate the time sound travelled in water before transmitted through the water–sediment interface (see Fig. 1 for an example of acoustic propagation path). With in-sediment propagation distance and time, the total travel time less the time traveled in water, sediment sound speed was calculated through the time-of-flight method. Sediment sound speed was calculated for all source–receiver pairs and waveforms in the 1–10 kHz band. Note, refraction at the water–sediment interface was not included in the calculation of the travel distances. Given the grazing angle range of 45°–68° and sources 5–20 cm from the water–sediment interface, the difference in travel distance with or without refraction at the water–sediment interface is a fraction of a centimeter.

Estimates of sediment sound speed are shown in Fig. 7, where the most reliable results are in the frequency band of 2–8 kHz. For frequencies lower than 2 kHz, both the ITC1007 and ITC1032 have too low a source level, resulting in relatively large uncertainty. For frequencies higher than 8 kHz, data indicate possible multipath issues. The cause of the multipath at these higher frequencies remains to be understood, so results are somewhat uncertain. In the band of 2–8 kHz, sediment sound speed from all sites has an overall variation of 50 m/s at 2 kHz, and 80 m/s at 3–8 kHz. Transition1, the coarse sandy site, has the highest sound speed; the site near VLA1 with surficial mud has the lowest. Note, in Fig. 7, *VLA1mud* corresponds to the case that all sources were buried in mud, while *VLA1sand* is 20 m west of the *VLA1mud* location. Except for site WARBAL, all dispersion curves are monotonic with the highest dispersion of 3% at the sandy sites and 1% at the muddy sites. The uncertainty bounds (Fig. 10) are 0.4–2% in the band of 2–8 kHz. The uncertainty bounds correspond to one standard deviation from the mean sound speed using data from the ten sources and receiver pairs. The overall level of sediment sound speeds is consistent with their corresponding sediment types, i.e., higher sound speed for coarse sand and lower sound speed for muddy sediment.

B. Sediment Attenuation Results

The Sediment attenuation coefficient is obtained by comparing the amplitudes of in-water and in-sediment data. Specifically, the envelope peaks of both in-water and in-sediment data are used. A different method (not shown here) that uses the integrated energy over a 3-dB width of the signal was also applied to data and yielded similar results as those presented here.

All TREX13 data were taken with the receiver at 3 m, as were the in-water data. Assuming the transmitted signal has an amplitude *A*, the received amplitude in water is $A_w = A/r$, where *r* is the total propagation distance between source and receiver. Assuming the sediment is a homogeneous fluid half-space, the received signal amplitude for in-sediment data is approximately $A_s = ((AT)/r)\, e^{-\alpha r_2}$, where α is the sediment attenuation coefficient in nepers per meter, r_2 is the propagation distance in sediment, and *T* is the transmission coefficient for a particular path. Sediment attenuation α' in decibel per meter can then be obtained by comparing the amplitudes of in-water and in-sediment data, A_w and A_s, as follows [15]:

$$\alpha' = 8.686 * \alpha = 8.686 * \frac{\log_{10}\left(T\frac{A_w}{A_s}\right)}{r_2 \log_{10} e}. \tag{1}$$

There are two assumptions made in (1). One assumption is that there is negligible refraction. The other is the unknown transmission coefficient *T*, whose value depends on sediment sound speed, attenuation, density, and grazing angle. To quantify the effects of both assumptions to obtain attenuation, an exact solution, a wavenumber integration method [15], was used to simulate the in-sediment data with a half-space fluid model.

True geometries of the ten source–receiver pairs on SAMS were used in the simulation. For TREX13 data, with all measurements conducted at 3 m depth, the grazing angle range of all paths is 45°–68°. For each source–receiver pair, i.e., one grazing angle, ranges of sediment properties are given to simulate the resultant uncertainty in transmission coefficient *T*. Sediment sound speed is given a range of 1580–1700 m/s, attenuation 0.1–5 dB/m, and density 1.6–2.2 g/cm^3. For the grazing angle range of 45°–68°, the transmission coefficient is in the well-defined range of 1.22 ± 0.06, which represents the combined effect of refraction and unknown *T*. This, in turn, results in an additional $\pm$ 0.1 dB/m uncertainty in attenuation coefficients if (1) is used. The additional uncertainty is incorporated in the attenuation results presented in this paper.

Note, for the VLA1 mud case where all sources are buried, a slightly different formula was used to calculate sediment attenuation

$$\alpha' = 8.686 * \alpha = 8.686 * \frac{\log_{10}\left(\frac{A_w}{A_s}\right)}{r \log_{10} e} \tag{2}$$

where *r* is the total propagation distance. For this buried case, direct comparison of in-water and in-sediment signal amplitudes was used, which does not involve the transmission coefficient.

The sediment attenuation coefficients from the five sites are shown in Fig. 8. These results represent attenuation averaged over the top 3 m of sediments along the main reverberation track. As with sound speed results, for frequency lower than 2 kHz, the attenuation coefficient flattens due to low source level. In the frequency band of 2–8 kHz, the coarse sandy site exhibits the highest attenuation, ranging 0.5–3.3 dB/m; for the VLA1 mud case where all sources are buried, results

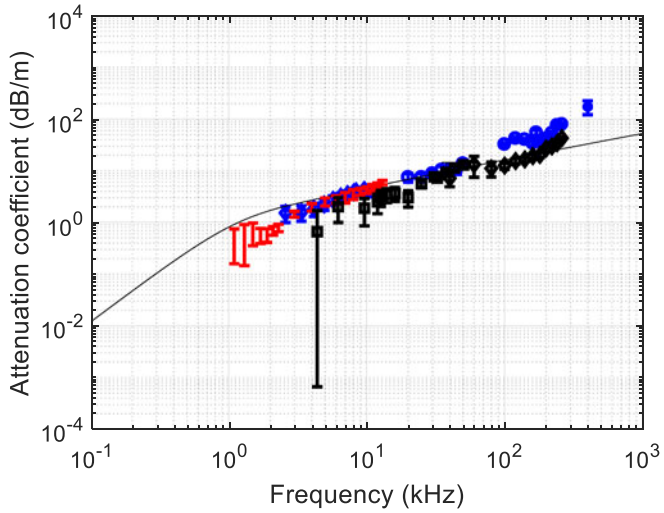

Fig. 11. Comparison of sediment attenuation among TREX13 (red, Transition1 site), SAX99 (blue), and SAX04 (black). Transition1 is the closest in terms of sediment properties to those of SAX99 and SAX04.

show the least frequency dependence: the sediment attenuation coefficient varies only from 0.5 to 1.0 dB/m for the same band. The remaining four sites, representing fine sand, sand/mud mixture, and complex bottom structure, have similar attenuation coefficients. A straight line, $\alpha' = 0.42 * f^1$, is shown as a reference in Fig. 8.

Cross comparisons among sites are shown in Fig. 9. VLA2, the site with homogeneous fine sand, is used as a reference in the comparisons. In Fig. 9(a) the three most distinctive sites are compared: coarse sand at Transition1, fine sand at VLA2, and buried in mud case at VLA1mud. The spread represents the surficial attenuation coefficient variation along the main reverberation track at the TREX13 site. The results at VLA2 are in general lower by 1 dB/m than at Transition1. For the two fine sand sites, MORAY and VLA2 [see Fig. 9(b)], the attenuation coefficients have overlapping uncertainty bounds in the frequency band of 3–10 kHz. In this band, the uncertainty bounds for MORAY are about twice those from the VLA2 site. The penetration rate data at the two sites [see Fig. 4(d) and (e)] indicate, though similar in surficial sediment properties, that the MORAY site has a more consolidated bottom beyond the surficial 1 m, which may contribute to the larger uncertainty bounds.

The WARBAL site has a more complicated bottom structure and is in a transition region with corrugation to without corrugation. Its attenuation coefficients, shown in Fig. 9(c), are slightly higher than those at VLA2 for 2–8 kHz and in general have larger uncertainty bounds. Fig. 9(d) shows the comparison between VLA2 and VLA1sand, which is 20 m west of the buried mud case with a bottom of sand/mud mixture. Interestingly, the attenuation coefficients at the two sites are very similar across the entire 1–10-kHz band.

C. Comparison With Other In Situ Measurements

Sediment sound speed and attenuation results at TREX13 are compared with results of *in situ* measurements conducted during the Sediment Acoustic Experiments in 1999 and 2004 (SAX99 and SAX04), both of which were carried out off Fort Walton Beach, FL, USA [1], [2], about 100 km northwest of the TREX13 site. The compiled sediment sound speed and attenuation results are shown in Figs. 10 and 11 with Biot theory predictions superimposed (see [1] for Biot parameters). The Biot parameters are either measured or modeled, fitting the Fort Walton conditions.

For sound speed ratio, results from TREX13 are consistently lower than those from SAX99 (Fig. 10). Among the five sites at TREX13, Transition1 is the closest in terms of sediment properties to those of SAX99 and SAX04. The sound-speed ratio at Transition1 (the top curve of TREX13 with circles) is 4% lower than that from SAX99 at 3 kHz. However, Transition1 results compare well with those reported by the Defense Research and Development Canada (DRDC) in SAX04 [2]. The comparison of sediment attenuation coefficients among TREX13 Transition1 site, SAX99, and SAX04 is shown in Fig. 11. The TREX13 attenuation coefficient at the coarse sandy site is close to that observed in SAX99 in the frequency band of 2–10 kHz. In this frequency band, SAX04 has limited data to compare to the two sites and the available attenuation coefficients are slightly lower than those from TREX13 Transition1 and SAX99.

IV. Summary

One of the reasons the TREX13 site was chosen was the seeming simplicity of bottom properties: Before detailed environmental measurements, the site was deemed a sandy site with minimal range and depth dependency. The SAMS data, along with the chirp and multibeam survey data, reveal a rather complex picture of the geoacoustic structure. The SAMS results, which are averages over the top 3 m of sediments, are consistent with that overall sediment structure inferred from the multibeam and chirp survey and provide quantitative data at the five representative sites. The chirp/multibeam survey and SAMS measurements will help in the development of a comprehensive geoacoustic models of sound propagation and reverberation at the site.

The multibeam bathymetric survey shows a series of bottom corrugations as well as their gradual disappearance along the 7-km main reverberation track [13]. Specifically, corrugations are clearly observed for the first 3 km and diminish down the track. Surficial sediment type changes as one follows the corrugations: from coarse sand on the ridges to soft mud over sand in the swales. After the disappearance of the corrugations, surficial sediment transitions into fine sand.

SAMS operation during TREX13 was designed to sample varying sediment types along the main reverberation track. Five sites were selected to cover 1) sediment properties on a ridge (Transition1) and in a swale (VLA1) where corrugation exists; 2) fine sand after the disappearance of corrugation (VLA2 and MORAY); and 3) the transition between the first two (WARBAL).

Sediment sound speeds from the five sites differ about 80 m/s between the highest (coarse sand) and the lowest (mud over sand) in the frequency band of 2–8 kHz. Dispersion is most pronounced (about 3%) at the sandy sites and the least at the muddy site (about 1%). Along the main reverberation track, there are two types of sand: coarse sand as seen on the sandy ridges (Transition1) and fine sand as seen at VLA2 and MORAY sites. Sound speed differs about 30–40 m/s between them.

The sediment attenuation coefficient is highest at the coarse sandy site, and lowest at the site with mud over sand. Transition1 attenuation varies from 0.5 to 3.3 dB/m in the frequency range of 2–8 kHz; at the mud site, attenuation varies little with frequency from 2 to 6 kHz at 0.5 dB/m to about 1.0 dB/m at 8 kHz. Interestingly, the rest of the measurements, given their different sediment types and properties, yield consistent attenuation coefficients, $\sim$0.3–2.8 dB/m from 2 to 8 kHz.

Both sediment sound speed ratio and attenuation coefficient were compared with those from SAX99 and SAX04. Sediment sound speed ratio at Transition1, the site that is closest in bottom properties to

SAX99 and SAX04, is in general lower than SAX99 by about 4% but compares well with SAX04 DRDC results. Attenuation at Transition1 compares well with SAX99 data in the frequency band of 2–10 kHz.

Summarizing the findings from the SAMS data, the following conclusions are made.

1) At the ridges within the first three kilometers of the track, the sediments are made of coarse sand represented by data from Transition1, where sound speed is the highest and the dispersion is the greatest. At the swales such as at the VLA1 site, the top portion of the sediment is made of mud with varying thickness and sand underneath. The measured sound speed is understood as an average of those of mud and sand, and found to be considerably lower than those at the ridges.
2) In between the ridges and swales, a viable assumption is that the surficial sound speed is smoothly transitional. The validity of this assumption needs to be confirmed by either additional measurements or inferring from other TREX13 acoustic data.
3) Beyond the first 3 km, the sediment is more consistent with fine sand (VLA2 and MORAY), where the sound speed is slightly lower than on the ridges.
4) The sediment attenuation coefficient is the highest on the sand ridges and lowest in the swales. At other sites, in between sand ridges and swales, and in the fine sand area further down the main reverberation track (VLA1sand, WARBAL, VLA2, and MORAY), attenuation coefficient is observed to be similar in value, although their sediment types and properties differ.
5) The sound speed and attenuation measured by SAMS should be understood as an average over the top 3 m of sediments in the frequency band of 2–8 kHz. Depth varying properties were not measured. To do so would have required taking measurements at several depths between 0 and 3 m, but the time requirement for this was too great for the experiment. For the purpose of developing geoacoustic models in the TREX13 site, SAMS data should be used to constrain the models, i.e., these geoacoustic models should be consistent with the SAMS data for the surficial 3 m of sediments.

ACKNOWLEDGMENT

The authors thank the engineering team of V. Miller, N. Michel-Hart, B. Brand, P. Aguilar, M. Kenney, and E. Boget at APL-UW for the design, assembly, and testing of SAMS. They also thank K. L. Williams and B. T. Hefner at APL-UW for valuable discussions and for providing SAX99 and SAX04 data. The authors thank the *R/V Sharp* crew for support during the experiment.

REFERENCES

[1] K. L. Williams, D. R. Jackson, E. I. Thorsos, D. Tang, and S. G. Schock, "Comparison of sound speed and attenuation measured in a sandy sediment to predictions based on the Biot theory of porous media," *IEEE J. Ocean. Eng.*, vol. 27, no. 3, pp. 413–428, Jul. 2002.

[2] P. C. Hines, J. C. Osler, J. G. E. Scrutton, and L. J. S. Halloran, "Time-of-flight measurements of acoustic wave speed in a sandy sediment at 0.6–20 kHz," *IEEE J. Ocean. Eng.*, vol. 35, no. 3, pp. 502–515, Jul. 2010.

[3] E. L. Hamilton, G. Shumway, H. W. Menard, and C. J. Shipek, "Acoustic and other physical properties of shallow-water sediments off San Diego," *J. Acoust. Soc. Amer.*, vol. 28, pp. 1–15, 1956.

[4] A. Turgut and T. Yamamoto, "Measurements of acoustic wave velocities and attenuation in marine sediments," *J. Acoust. Soc. Amer.*, vol. 87, pp. 2376–2383, 1990.

[5] A. I. Best, Q. J. Huggett, and A. J. K. Harris, "Comparison of in situ and laboratory acoustic measurements on Lough Hyne marine sediments," *J. Acoust. Soc. Amer.*, vol. 110, pp. 695–709, 2001.

[6] G. B. N. Robb *et al.*, "Measurements of the in situ compressional wave properties of marine sediments," *IEEE J. Ocean. Eng.*, vol. 32, no. 2, pp. 484–496, Apr. 2007.

[7] A. Barbegelata *et al.*, "ISSAMS: An in situ sediment acoustic measurement system," in *Shear Waves in Marine Sediments*, J. M. Hoven, M. D. Richardson, and R. D. Stoll, Ed., Dordrecht, The Netherlands: Kluwer, 1991.

[8] M. D. Richarson, D. L. Lavoie, and K. B. Briggs, "Geoacoustic and physical properties of carbonate sediments of the lower Florida Keys," *Geo-Mar. Lett.*, vol. 17, pp. 316–324, 1997.

[9] M. J. Buckingham and M. D. Richardson, "On tone-burst measurements of sound speed and attenuation in sandy marine sediments," *IEEE J. Ocean. Eng.*, vol. 27, no. 3, pp. 429–453, Jul. 2002.

[10] S. S. Fu, R. H. Wilkens, and L. N. Frazer, "Acoustic lance: New in situ seafloor velocity profiles," *J. Acoust. Soc. Amer.*, vol. 99, pp. 234–242, 1996.

[11] M. S. Ballard, K. M. Lee, A. R. McNeese, and P. S. Wilson, "Development of a system for in situ measurements of geoacoustic properties during sediment coring," *J. Acoust. Soc. Amer.*, vol. 139, pp. 2125–2125, 2016.

[12] J. Yang, D. Tang, and K. L. Williams, "Direct measurement of sediment sound speed in Shallow Water'06," *J. Acoust. Soc. Amer.*, vol. 124, 2008, Art. no. EL116-EL121.

[13] C. de Moustier, "Multibeam bathymetric survey for the Target and Reverberation Experiment 2013," *IEEE J. Ocean. Eng.*, 2017, to be published.

[14] J. A. Goff, "Seismic and core investigation off Panama City, Florida, reveals sand ridge influence on formation of the shoreface ravinement," *Continental Shelf Res.*, vol. 88, pp. 34–46, 2014.

[15] F. B. Jensen, W. A. Kuperman, M. B. Porter, and H. Schmidt, *Computational Ocean Acoustics*. New York, Ny, USA: AIP Press, 1994, pp. 33–34.

Jie Yang received the B.S. degree in physics from the Ocean University of Qingdao, Qingdao, China, in 1999 and the Ph.D. degree in mechanical engineering from the Georgia Institute of Technology, Atlanta, GA, USA, in 2007.

Since 2007, she has been a Postdoctoral Fellow supported by the U.S. Office of Naval Research and then a Physicist with the Applied Physics Laboratory, University of Washington, Seattle, WA, USA. Her research interests include both active and passive acoustics, with the former focusing on midfrequency sound propagation and reverberation in littoral oceans and the latter on estimating wind speed and rain rate using ocean ambient sound and their relation to global water cycle and climate change.

Dr. Yang is a member of the Acoustical Society of America.

Dajun Tang received the B.S. degree in physics from the University of Science and Technology, Hefei, China, in 1981, the M.S. degree in physics and acoustics from the Institute of Acoustics, Beijing, China, in 1985, and the Ph.D. degree in oceanographic engineering from the Joint Program of Massachusetts Institute of Technology, Cambridge, MA, USA, and the Woods Hole Oceanographic Institution, Woods Hole, MA, USA, in 1991.

From 1991 to 1996, he was first an Assistant Scientist and then an Associate Scientist at Woods Hole Oceanographic Institution. In 1996, he joined the Applied Physics Laboratory, University of Washington, Seattle, WA, USA, where he is currently a Principal Senior Oceanographer. His research interests include acoustics in shallow water, including both field experiments and modeling. His current concentration is in the area of environmental impact on midfrequency reverberation.

Dr. Tang was Co-Chief Scientist for the Shallow Water 2006 experiment and the Target and Reverberation Experiment. He is a Fellow of the Acoustical Society of America.